

LINEAR STABILITY ANALYSIS OF ESCARPMENT PLANFORMS BY GROUNDWATER SAPPING

Adichai PORNPROMMIN¹ and Norihiro IZUMI²

¹Member of JSCE, D.Eng., Lecturer, Dept. Water Resources Engineering, Kasetsart University
(50 Phaholyothin Rd., Jatujak, Bangkok 10900, Thailand)

²Member of JSCE, Ph.D., Professor, Dept. Civil Engineering, Hokkaido University
(Kita 13 Nishi 8, Kita-ku, Sapporo, Hokkaido 060-8628, Japan)

The planimetric outlines of escarpments can be used to characterize many landforms. The retreat speed of a scarp is influenced by three main processes, scarp backwasting, fluvial incision and groundwater sapping. In this study, we performed a linear stability analysis of the planimetric outlines by considering the processes of scarp backwasting and groundwater sapping. The retreat speed of the scarp due to backwasting is assumed to be a function of the scarp curvature in which convexity will enhance the rate of retreat, whereas the retreat speed due to groundwater sapping is a function of water discharge. We found that, if the retreat speed depends on water discharge alone, no dominant channel spacing can be found. With an increase of the effect of scarp curvature, dominant channel spacing becomes larger. Thus, the self-organized channels can be modeled if the proper treatment of the effect of scarp curvature is taken into account.

Key Words : *Linear stability analysis, channelization, groundwater sapping.*

1. INTRODUCTION

Escarpment is a steep slope or long cliff that separates two areas of different levels. Thus, many landforms can be well characterized by the planimetric outlines of escarpments. There are various shapes of the planforms of escarpments such as reentrants, rounded projections and sharply pointed projections. According to *Howard and Selby*¹⁾, the scarp form can be determined by the spatial distribution of erosion and by lithologic and structural influences such as rock thickness and dip. As escarpments are created by lateral retreat of scarps, *Howard*²⁾ proposed three major processes of scarp retreat as follows: scarp backwasting, fluvial incision and groundwater sapping. Scarp backwasting is termed as erosion of the scarp face by rockfall, slumping, undermining and weathering. Fluvial erosion creates downcutting by streams which originate on the top of the escarpment and pass over the front of the escarpment, whereas groundwater sapping is the process that undercuts or undermines a scarp induced by seepage erosion.

In this study, we perform a linear stability analysis to investigate the characteristics of

escarpment planforms. Two major processes, scarp backwasting and groundwater sapping, are considered, and the results are compared with the experimental results of *Pornprommin and Izumi*³⁾. If the planimetric outline of escarpments is unstable, it is assumed to trigger channelization, and a channel network may develop afterward.

2. FORMATION

(1) Groundwater Flow Equation

Let us consider groundwater flow in an unconfined aquifer with a free water surface above an inclined impermeable layer as shown in Figure 1. If the gradients of the piezometric surface are assumed to be sufficiently small, the pressure distribution can be approximated to be hydrostatic, and the movement of groundwater flow can be described by the following Dupuit-Forchheimer equation:

$$\frac{1}{\phi} \frac{\partial \tilde{h}}{\partial \tilde{t}} - \frac{\partial}{\partial \tilde{x}} \left[\tilde{K} \tilde{h} \left(\frac{\partial \tilde{h}}{\partial \tilde{x}} - S \right) \right] - \frac{\partial}{\partial \tilde{y}} \left(\tilde{K} \tilde{h} \frac{\partial \tilde{h}}{\partial \tilde{y}} \right) = 0 \quad (1)$$

where $\tilde{}$ denotes the dimensional variables, \tilde{t} is time, \tilde{x} and \tilde{y} are the streamwise and lateral

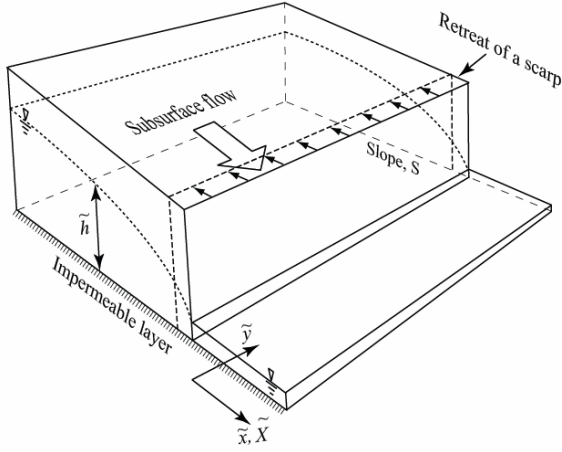


Fig.1 Scarp (seepage face) and groundwater flow.

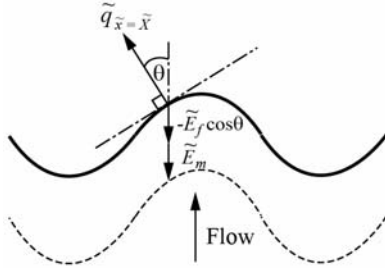


Fig.2 Retreat speed of a scarp.

directions respectively, \tilde{h} is water depth, \tilde{K} is the hydraulic conductivity, ϕ is porosity, and S is the slope of the impermeable layer.

(2) Retreat speed of a scarp

As shown in Figure 2, the retreat speed of a scarp (seepage face) in the \tilde{x} direction is assumed to be described as follows:

$$\frac{\partial \tilde{X}}{\partial \tilde{t}} = -\tilde{E}_f \cos \theta + \tilde{E}_m \quad (2)$$

where \tilde{X} denotes the location of the scarp which is a function of \tilde{y} and \tilde{t} , \tilde{E}_f is the retreat speed due to groundwater flow which can be expressed in an exponential function of the water discharge at the scarp [Howard²⁾] as follows:

$$\tilde{E}_f = \tilde{\alpha} \left(\frac{\tilde{q}_{\tilde{x}=\tilde{X}} - \tilde{q}_{th}}{\tilde{q}_r} \right)^\gamma \quad (3)$$

where $\tilde{q}_{\tilde{x}=\tilde{X}}$, \tilde{q}_r and \tilde{q}_{th} are the unit discharge at the scarp, the reference unit discharge and the threshold unit discharge respectively, $\tilde{\alpha}$ is an empirical constant with the dimension of velocity, and γ is a dimensionless exponent. The unit water discharge \tilde{q} is expressed as

$$\tilde{q} = (\tilde{u}^2 + \tilde{v}^2)^{1/2} \tilde{h} \quad (4)$$

where \tilde{u} and \tilde{v} are the velocity components in the \tilde{x} and \tilde{y} directions respectively and assumed to be uniform in the vertical direction as follows:

$$(\tilde{u}, \tilde{v}) = \left(-\tilde{K} \left(\frac{\partial \tilde{h}}{\partial \tilde{x}} - S \right), -\tilde{K} \frac{\partial \tilde{h}}{\partial \tilde{y}} \right) \quad (5)$$

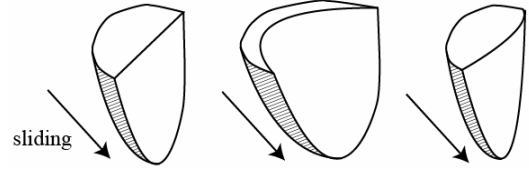


Fig.3 Effect of scarp convexity on backwasting.

The angle between the \tilde{x} direction and groundwater flow normal to the scarp face θ is used to calculate the retreat speed in the \tilde{x} direction, such that

$$\cos \theta = 1 / \sqrt{1 + \left(\frac{\partial \tilde{X}}{\partial \tilde{y}} \right)^2} \quad (6)$$

According to Howard²⁾, the retreat speed of the scarp due to backwasting \tilde{E}_m can be assumed to be uniform as the first approximation. However, he mentioned that the mechanism will be enhanced by scarp convexity. For example, in Figure 3, the right block with a convex planimetric outline has a higher possibility of backwasting than others. Thus, for simplicity, we assumed that it can be expressed by a diffusion function as follows:

$$\tilde{E}_m = \tilde{\varepsilon} \frac{\partial^2 \tilde{X}}{\partial \tilde{y}^2} \quad (7)$$

where $\tilde{\varepsilon}$ denotes the curvature coefficient of the planimetric outline of a scarp influencing the magnitude of the retreat speed due to backwasting.

(3) Boundary conditions

Suppose that the sediment layer extended from the seepage face to far upstream. The seepage flow will reduce to a constant, laterally uniform flow far upstream. Thus, the boundary conditions far upstream can be written as

$$(\tilde{u}, \tilde{v}) = (\tilde{K}S, 0), \quad \tilde{h} = \tilde{H}_{-\infty} \quad \text{as } \tilde{x} \rightarrow -\infty \quad (8)$$

where $\tilde{H}_{-\infty}$ denotes the constant water depth far upstream. If there is no reservoir downstream of the scarp, the groundwater depth at the scarp will be almost zero. If the groundwater depth is zero, the groundwater velocity, however, becomes infinity in the Dupuit approximation in which it will violate our analysis. As a result, non-zero value of water depth is necessary to be assumed at the seepage face. Let us consider the constant water depth at the scarp (seepage face) \tilde{h}_e , and, thus, the boundary condition at the scarp can be written as

$$\tilde{h} = \tilde{h}_e \quad \text{at } \tilde{x} = \tilde{X} \quad (9)$$

(4) Normalization

The following transformations are introduced, in which the variables without tildes are the normalized version of the corresponding variables with tildes:

$$(\tilde{x}, \tilde{y}, \tilde{X}) = \frac{\tilde{H}_{-\infty}}{S} (x, y, X), \quad \tilde{h} = \tilde{H}_{-\infty} h \quad (10a,b)$$

$$\tilde{t} = \frac{\tilde{H}_{-\infty}}{S\tilde{\alpha}} t, \quad \tilde{q}_r = \tilde{K}\tilde{S}\tilde{H}_{-\infty} \quad (10c,d)$$

With the use of the above normalization (10a–d), the governing equations (1) and (2) are rewritten as

$$\frac{1}{\beta} \frac{\partial h}{\partial t} + \frac{\partial h}{\partial x} - \frac{\partial}{\partial x} \left(h \frac{\partial h}{\partial x} \right) - \frac{\partial}{\partial y} \left(h \frac{\partial h}{\partial y} \right) = 0 \quad (11)$$

$$\frac{\partial X}{\partial t} = -E \cos \theta + \varepsilon \frac{\partial^2 X}{\partial y^2} \quad (12)$$

where the normalized fluvial erosion due to seepage flow is

$$E = \left[\left\{ \left(1 - \frac{\partial h}{\partial x} \right)^2 + \left(\frac{\partial h}{\partial y} \right)^2 \right\}^{1/2} h - \psi \right]^\gamma \quad (13)$$

In (11), the parameter β indicates the relationship between subsurface flow velocity and seepage erosion as

$$\beta = \frac{\phi \tilde{K} S}{\tilde{\alpha}} \quad (14)$$

In (12), the normalized curvature parameter ε is

$$\varepsilon = \frac{\tilde{\varepsilon}}{\tilde{\alpha}} \quad (15)$$

which implies the relative magnitude of the retreat of a scarp by backwasting to that by seepage flow. In (13), ψ denotes the ratio between the threshold water discharge for seepage erosion and water discharge as follows:

$$\psi = \frac{\tilde{q}_{th}}{\tilde{K}\tilde{S}\tilde{H}_{-\infty}} \quad (16)$$

where $0 \leq \psi < 1$.

The boundary conditions (8) and (9) are normalized as

$$h = 1 \quad \text{as } x \rightarrow -\infty \quad (17)$$

$$h = h_\varepsilon \quad \text{at } x = X \quad (18)$$

where $0 < h_\varepsilon < 1$.

(5) Coordinate transformation

Considering the base state of the problem in which the seepage face retreats at a constant speed, the variables such as water depth and velocity can be considered steady under the proper moving coordinates as follows:

$$t^* = t, \quad x^* = x - X_0 \quad (19a,b)$$

where $*$ denotes the moving coordinates, and X_0 is the location of the scarp surface in the base state and a function of time t .

From (19), the following relations are derived:

$$\frac{\partial}{\partial t} = \frac{\partial t^*}{\partial t} \frac{\partial}{\partial t^*} + \frac{\partial x^*}{\partial t} \frac{\partial}{\partial x^*} = \frac{\partial}{\partial t^*} - \frac{dX_0}{dt} \frac{\partial}{\partial x^*} \quad (20a)$$

$$\frac{\partial}{\partial x} = \frac{\partial t^*}{\partial x} \frac{\partial}{\partial t^*} + \frac{\partial x^*}{\partial x} \frac{\partial}{\partial x^*} = \frac{\partial}{\partial x^*} \quad (20b)$$

Substituting (20a,b) into (11)–(12) and reducing, we obtain

$$\frac{1}{\beta} \frac{\partial h}{\partial t} + (f+1) \frac{\partial h}{\partial x} - \frac{\partial}{\partial x} \left(h \frac{\partial h}{\partial x} \right) - \frac{\partial}{\partial y} \left(h \frac{\partial h}{\partial y} \right) = 0 \quad (21)$$

$$\frac{\partial X}{\partial t} = -E \cos \theta + \varepsilon \frac{\partial^2 X}{\partial y^2} \quad (22)$$

where $*$ is dropped for simplicity, and the parameter f is

$$f = -\frac{1}{\beta} \frac{dX_0}{dt} \quad (23)$$

and dX_0/dt denotes a constant retreat speed of the scarp in the base state.

3. ONE-DIMENSIONAL BASE STATE

In the one-dimensional base state, the governing equation (21) is reduced to

$$(f+1) \frac{dh_0}{dx} - \frac{d}{dx} \left(h_0 \frac{dh_0}{dx} \right) = 0 \quad (24)$$

and the retreat speed of the scarp (22) becomes

$$\frac{dX_0}{dt} = -E_0, \quad E_0 = \left[\left(1 - \frac{dh_0}{dx} \right) h_0 - \psi \right]^\gamma \quad (25)$$

where the subscript 0 denotes the one-dimensional base state solution.

Integrating (24) and using the boundary condition far upstream (17), we obtain

$$\frac{dh_0}{dx} = -(f+1) \frac{1-h_0}{h_0} \quad (26)$$

Again, integrating (26) and using the condition at the scarp face (18), we obtain the relation between x and h_0 as follows:

$$x = \frac{1}{f+1} \left[(h_0 - h_\varepsilon) + \ln \left(\frac{1-h_0}{1-h_\varepsilon} \right) \right] \quad (27)$$

Substituting (23) and (26) into (25), the parameter f can be estimated by

$$h_\varepsilon = 1 - \frac{(\beta f)^{1/\gamma} + \psi - 1}{f} \quad (28)$$

4. TWO-DIMENSIONAL PERTURBATION PROBLEM

We introduce the following expansions:

$$(h, X) = (h_0(x), X_0(t)) + A(h_1(x), X_1) e^{\Omega t} \cos ky \quad (29)$$

where the subscript 1 denotes the linear solution, A is a small amplitude, Ω is the growth rate of perturbation, k is the wave number of perturbation, X_1 is a constant, and h_1 is a function of x .

Substituting (29) into (21) and (22) and reducing, at $O(A)$, we obtain

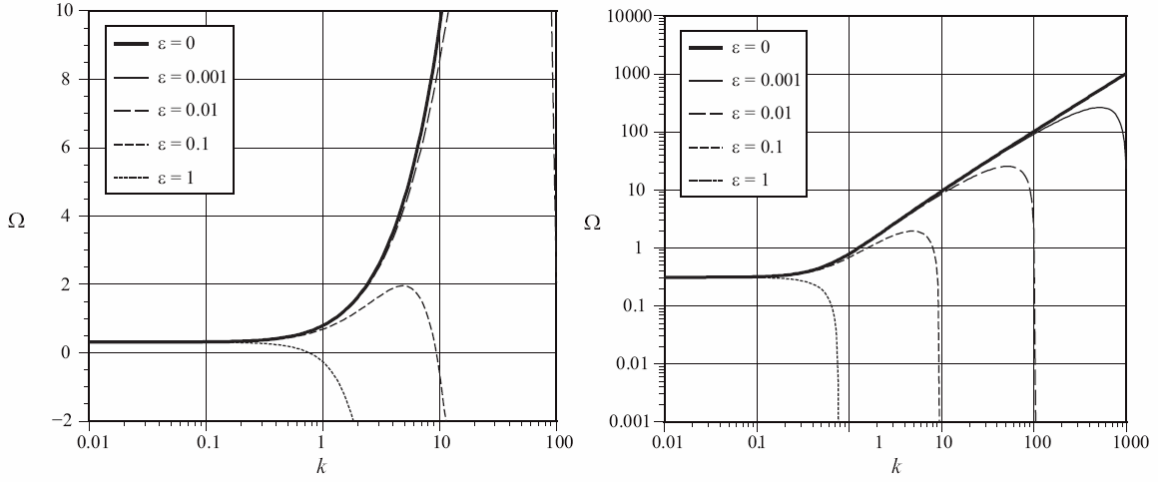


Fig.4 The growth rate of perturbation Ω as a function of k and ε for $\beta = 10$, $\gamma = 1.5$ and $h_\varepsilon = 0.4$.

In the left figure, Ω is in the linear scale. In the right figure, Ω is in the logarithmic scale.

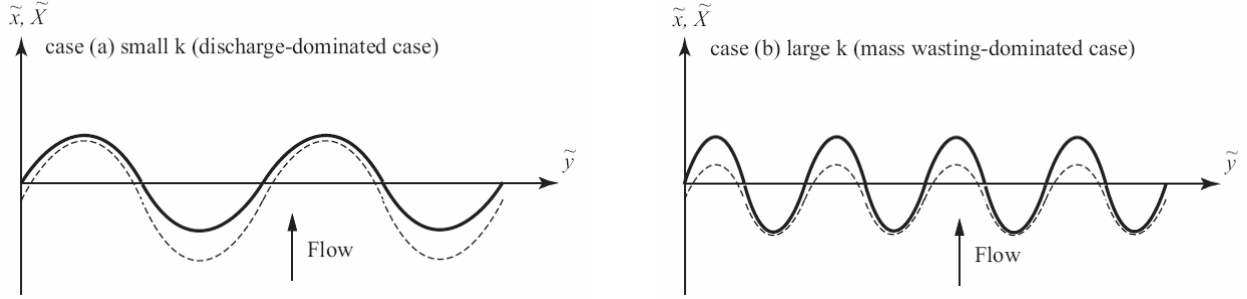


Fig.5 Concept of the retreat speed affected by the fluvial and mass-wasting processes.

Solid lines are the initial perturbations, and dashed lines are the evolutions of perturbations.

$$-h_0 h_1'' + (f + 1 - 2h_0') h_1' + (\beta^{-1} \Omega + k^2 h_0 - h_0'') h_1 = 0 \quad (30)$$

$$\gamma E_0^{1-1/\gamma} (1 - h_0') h_1 - \gamma E_0^{1-1/\gamma} h_0 h_1' + (\Omega + k^2 \varepsilon) X_1 = 0 \quad (31)$$

where ' denotes the derivative with respect to x .

Equation (30) forms a second-order ordinary differential equation with an eigenvalue Ω which needs two boundary conditions in order to solve.

The first boundary condition can be found at far upstream where the perturbation should vanish. Thus,

$$h_1 = 0 \quad \text{as } x \rightarrow -\infty \quad (32)$$

At the downstream end where the scarp is located, the condition (18) becomes

$$h_1 + h_0' X_1 = 0 \quad \text{at } x = 0 \quad (33)$$

Eliminating X_1 by substituting (33) into (31) and reducing, we obtain the second boundary condition as follows:

$$\left(\frac{\Omega + k^2 \varepsilon}{h_0'} - \gamma E_0^{1-1/\gamma} (1 - h_0') \right) h_1 + \gamma E_0^{1-1/\gamma} h_0 h_1' = 0 \quad \text{at } x = 0 \quad (34)$$

Thus, the governing equation (30) with the boundary conditions (32) and (34) will be solved for the eigenvalue Ω by using the Chebyshev polynomial method [Boyd⁴].

5. RESULTS AND DISCUSSION

Figure 4 shows the characteristics of the growth rate of perturbations Ω with varying the wave number k and the parameter ε indicating the influence of the curvature of the scarp face to the retreat speed by backwasting. While k is shown in the logarithmic scale, Ω is shown in the linear and logarithmic scales in the left and right figures, respectively. If $\varepsilon = 0$, it implies that the retreat speed depends on water discharge only. It is found that, without the effect of scarp curvature, Ω increases linearly with an increase of k . Thus, no characteristic channel spacing can be found for this extreme case. Howard⁵ found this shortcoming, so he resolved the problem by imposing a random function on the hydraulic conductivity \tilde{K} . Thus, the channel spacing in his model was found to depend on the inputs of the model grid scale and the random function. In this study, if we apply non-zero value to the scarp curvature parameter ε , it is found that Ω does not change in the range of very small k but decreases abruptly in the ranges of sufficiently large k . Thus, the dominant wave number k_{\max} corresponds to the maximum growth

Table 1 Estimation of the dominant wave number k_{\max} and the curvature parameter ε .

Chamber Slope S	Water Depth $\tilde{H}_{-\infty}$ (cm)	Channel Spacing \tilde{L} (cm)	Wave Number k	β	h_ε	ε
0.053	4.19	150	3.33	1.90	0.041	0.10
0.107	2.08	120	1.01	3.87	0.083	0.25
0.161	1.38	100	0.54	5.80	0.124	0.36
0.214	1.04	86	0.36	7.70	0.165	0.41
0.266	0.84	75	0.26	9.57	0.205	0.43
0.317	0.70	67	0.21	11.41	0.244	0.44
0.367	0.61	60	0.17	13.22	0.283	0.44

rate of perturbations Ω_{\max} can be estimated in the case of non-zero value of ε . From the figures, if $\varepsilon = 0.001, 0.01$ and 0.1 , k_{\max} are approximately 500, 50, and 5, respectively. Thus, the effect of curvature constrains the channelization with large k (small channel spacing), and k_{\max} decreases with an increase of the scarp curvature parameter ε .

Figure 5 represents the conceptual diagrams of the effects of the fluvial and mass-wasting processes to the retreat of the scarp. Small amplitude sinusoidal perturbations with varying wave number k are introduced at the scarp in the figure. In case (a), the perturbation with small wave number k (large channel spacing) is assumed to be imposed on the scarp. Due to large channel spacing, the effect of curvature becomes small. Thus, the retreat of seepage face is dominated by the fluvial process, and that the rate of scarp retreat of the inward outline is higher than the rate of the outward outline because of the concentration of water discharge. In contrast, the effect of curvature will be strong if the wave number of perturbation k is large as shown in case (b). Thus, the effect of mass wasting dominates the retreat of the scarp. The convex portion of the scarp (the outward outline of scarp) will be retreated with the rate higher than the concave portion (the inward outline). Therefore, with the use of this concept, we can investigate the self organizing channelization.

The result in Figure 4 suggests that, with the proper treatment of the curvature parameter ε , the self-organized channel can be generated without imposing a random function, and the model can be independent from a grid scale. Thus, we try to estimate ε using our experimental data³⁾. Table 1 shows the estimation of the dominant wave number k_{\max} and the curvature parameter ε corresponding to the results of our experiments. A sediment layer of

1.5m width, 1.2m length and 6-10cm thickness was created in a wooden chamber. The experiments had been conducted with varying the slope chamber S as shown in the first column of the table. The porosity ϕ of 0.3 and the hydraulic conductivity \tilde{K} of 10cm/s were measured, and a water discharge of 20liter/min was assumed. Thus, water depth far upstream $\tilde{H}_{-\infty}$ can be computed by $\tilde{Q}/\tilde{K}S\tilde{B}$ as shown in the second column. It is found that $\tilde{H}_{-\infty}$ decreases with an increase of the chamber slope S . The dominant channel spacing \tilde{L} from the experimental result for each slope S was shown in the third column. Thus, the dominant wave numbers k_{\max} in the fourth column were computed from

$$k_{\max} = \frac{2\pi\tilde{H}_{-\infty}}{S\tilde{L}} \quad (35)$$

Since k_{\max} is normalized with $\tilde{H}_{-\infty}$, it was found to decrease with an increase of S . In order to compute the parameter β , it is necessary to estimate the parameter $\tilde{\alpha}$ representing the retreat due to the fluvial erosion in (3). From the experiment, the initial scarp retreat speed \tilde{E}_{f_0} is roughly in the order of unity in the cm/min scale, and increases as headcutting progresses further upstream. As the first approximation, we assigned a constant value of 1cm/min to \tilde{E}_{f_0} . Thus, β can be estimated in the fifth column using (14). We assumed the Froude critical water depth as the water depth at the scarp \tilde{h}_ε . Thus, the relative water depth h_ε can be estimated in the sixth column. As the experiments were conducted with the water discharge slightly above the erosion threshold, ψ is assumed to be 0.8. Therefore, ε were finally estimated by matching the experiment results of k_{\max} with that from the linear

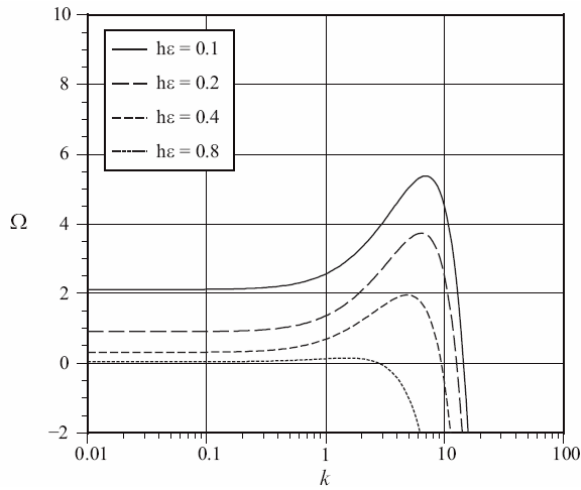


Fig.6 The growth rate of perturbation Ω as a function of k and h_ε for $\varepsilon = 0.1$, $\beta = 10$, $\psi = 0$ and $\gamma = 1.5$.

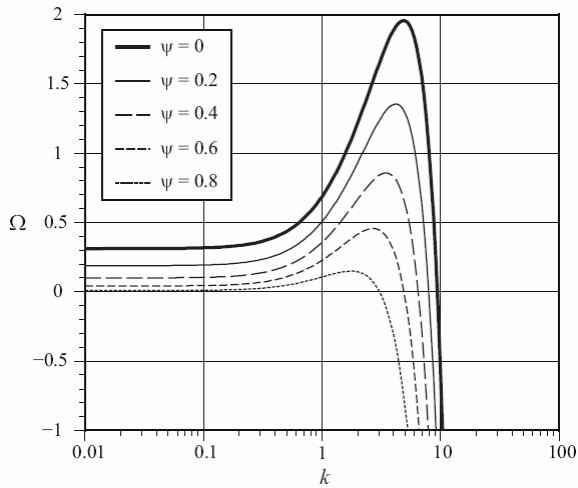


Fig.7 The growth rate of perturbation Ω as a function of k and ψ for $\varepsilon = 0.1$, $\beta = 10$, $\gamma = 1.5$ and $h_\varepsilon = 0.4$.

stability analysis as shown in the last column. We found that ε shows the values in the order of 0.1. In addition, the computation was repeated for a wide range of uncertain assumptions such as \tilde{E}_{f0} and \tilde{h}_ε , but it was found that ε does not change significantly.

Figure 6 shows the relation between the relative water depth h_ε to the growth rate of perturbations Ω . The parameter h_ε is the ratio of water depth at the scarp to water depth far upstream. It is found that Ω in the range of small and moderate wave number k and the dominant wave number k_{\max} increase with a decrease of h_ε . When h_ε decreases, it means that the difference between water levels at the scarp and far upstream increases, and that the gradient of piezometric head increases. Because of the high gradient, subsurface flow concentration should be amplified and may respond to an increase of the growth rate of perturbation Ω .

The effect of ψ which represents the ratio of the threshold water discharge to water discharge is shown in Figure 7. It is found that the growth rate of perturbations Ω in the range of moderate wave number k and the dominant wave number k_{\max} increase with a decrease of ψ . It implies that channelization with small spacing may develop if water discharge is well above the threshold erosion. The result corresponds well with the result from the experimental study by Howard⁵⁾ that, at high flow rates and with correspondingly more rapid erosion, the competition between adjacent channels becomes less pronounced, more main channels with smaller channel spacing are active.

6. CONCLUSION

A linear stability analysis was performed to investigate the characteristics of escarpment planforms that were eroded and retreated by groundwater sapping and backwasting. It was found that the convexity of the planimetric outline of escarpment is an important parameter that can indicate the self-organized channel spacing. In the case that the fluvial process is dominant, the perturbations will grow, whereas, in the case that the backwasting process with convexity-enhanced rate is dominant, the perturbations may decay. Using our previous experimental study, we found that the normalized curvature parameter ε is the order of 0.1. A decrease of water depth at the scarp and an increase of groundwater flow may induce more channels with smaller channel spacing.

ACKNOWLEDGMENT:

This work was supported by the Japan Society for the Promotion of Science Postdoctoral Fellowship Program (grant-in-aid P 07116).

REFERENCES

- 1) Howard, A. D. and Selby, M. J.: Rock slopes, *Geomorphology of Desert Environments*, Abrahams, A. D. and Parsons, A. J. eds., Chapman and Hall, London, pp.123-172, 1994.
- 2) Howard, A. D.: Simulation modeling and statistical classification of escarpment planforms, *Geomorphology*, Vol.12, pp.187-214, 1995.
- 3) Pornprommin, A and Izumi, N.: Experimental study of channelization by seepage erosion, *Journal of Applied Mechanics*, Vol.11, JSCE, pp.709-717, 2008.
- 4) Boyd, J. P.: *Chebyshev and Fourier Spectral Methods*, 2nd Ed., Dover, New York, 2001.
- 5) Howard, A. D.: Groundwater sapping experiments and modeling, in *Sapping Features of the Colorado Plateau: A Comparative Planetary Geology Field Guide*, edited by A. D. Howard, R. C. Kochel, and H. Holt, NASA Spec. Publ., SP-491, 71-83, 1988.

(Received September 30, 2008)